BRAIN
ORIGINAL ARTICLE

A genetic link between risk for Alzheimer's disease and severe COVID-19 outcomes via the *OAS1* gene

Naciye Magusali,[1,†] Andrew C. Graham,[1,†] Thomas M. Piers,[2] Pantila Panichnantakul,[1] Umran Yaman,[1] Maryam Shoai,[1,3] Regina H. Reynolds,[3,4,5] Juan A. Botia,[3,6] Keeley J. Brookes,[7] Tamar Guetta-Baranes,[8] Eftychia Bellou,[9] Sevinc Bayram,[10] Dimitra Sokolova,[1] Mina Ryten,[3,4,5] Carlo Sala Frigerio,[1] Valentina Escott-Price,[9] Kevin Morgan,[8] Jennifer M. Pocock,[2] John Hardy[1,3] and Dervis A. Salih[1]

[†]These authors contributed equally to this work.

Recently, we reported oligoadenylate synthetase 1 (*OAS1*) contributed to the risk of Alzheimer's disease, by its enrichment in transcriptional networks expressed by microglia. However, the function of *OAS1* within microglia was not known.
Using genotyping from 1313 individuals with sporadic Alzheimer's disease and 1234 control individuals, we confirm the *OAS1* variant, rs1131454, is associated with increased risk for Alzheimer's disease. The same *OAS1* locus has been recently associated with severe coronavirus disease 2019 (COVID-19) outcomes, linking risk for both diseases. The single nucleotide polymorphisms rs1131454(A) and rs4766676(T) are associated with Alzheimer's disease, and rs10735079(A) and rs6489867(T) are associated with severe COVID-19, where the risk alleles are linked with decreased *OAS1* expression. Analysing single-cell RNA-sequencing data of myeloid cells from Alzheimer's disease and COVID-19 patients, we identify co-expression networks containing interferon (IFN)-responsive genes, including *OAS1*, which are significantly upregulated with age and both diseases. In human induced pluripotent stem cell-derived microglia with lowered *OAS1* expression, we show exaggerated production of TNF-α with IFN-γ stimulation, indicating *OAS1* is required to limit the pro-inflammatory response of myeloid cells.
Collectively, our data support a link between genetic risk for Alzheimer's disease and susceptibility to critical illness with COVID-19 centred on *OAS1*, a finding with potential implications for future treatments of Alzheimer's disease and COVID-19, and development of biomarkers to track disease progression.

1 UK Dementia Research Institute at UCL, Gower Street, London WC1E 6BT, UK
2 Department of Neuroinflammation, Queen Square Institute of Neurology, UCL, London WC1N 1PJ, UK
3 Department of Neurodegenerative Diseases, Queen Square Institute of Neurology, UCL, London WC1N 1PJ, UK
4 NIHR Great Ormond Street Hospital Biomedical Research Centre, UCL, London WC1N 1EH, UK
5 Great Ormond Street Institute of Child Health, Genetics and Genomic Medicine, UCL, London WC1N 1EH, UK
6 Department of Information and Communications Engineering, Universidad de Murcia, 30100 Murcia, Spain
7 Biosciences, School of Science and Technology, Nottingham Trent University, Nottingham NG8 11NS, UK
8 Genetics, School of Life Sciences, Life Sciences Building, University Park, University of Nottingham, Nottingham NG7 2RD, UK
9 Dementia Research Institute, MRC Centre for Neuropsychiatric Genetics and Genomics, Cardiff University, Cardiff CF24 4HQ, UK
10 Hitachi Rail Europe Ltd, New Ludgate, London EC4M 7HX, UK

Received April 22, 2021. Revised July 19, 2021. Accepted August 02, 2021. Advance access publication October 7, 2021
© The Author(s) (2021). Published by Oxford University Press on behalf of the Guarantors of Brain.
This is an Open Access article distributed under the terms of the Creative Commons Attribution-NonCommercial License (https://creativecommons.org/licenses/by-nc/4.0/), which permits non-commercial re-use, distribution, and reproduction in any medium, provided the original work is properly cited. For commercial re-use, please contact journals.permissions@oup.com

Correspondence to: Dervis A. Salih
UK Dementia Research Institute at UCL
Gower Street, London WC1E 6BT, UK
E-mail: dervis.salih@ucl.ac.uk

Keywords: *OAS1*; Alzheimer's disease; COVID-19; microglia; interferon

Abbreviations: ARM = amyloid-responsive microglia; ARUK = Alzheimer's Research UK; COVID-19 = coronavirus disease 2019; DAM = disease-associated microglia; GWAS = genome-wide association studies; iPSC = induced pluripotent stem cell; IRM = interferon-response microglia; LD = linkage disequilibrium; scRNA-seq = single-cell RNA-sequencing; SNP = single nucleotide polymorphism

Introduction

Alzheimer's disease is not only characterized by extracellular amyloid-β deposits, tau tangles and neuronal death, but also extensive neuroinflammatory changes, which may push amyloid pathology to form tau tangles.[1–4] Genetic studies have revealed the importance of gene variants that alter risk for Alzheimer's disease and are expressed by the innate immune system, including *APOE*, *TREM2*, *CD33* and *PLCG2*.[5–7] Integrating genetic variants with RNA-sequencing (RNA-seq) and single-cell RNA-sequencing (scRNA-seq) approaches has begun to provide important new insights into the heterogeneous microglial activity changes in Alzheimer's disease progression, particularly in the identification of disease-associated microglia (DAM) or amyloid-responsive microglia (ARM).[8,9] This work generally postulates that many Alzheimer's disease risk genes, including *APOE*, *TREM2*, *CD33* and *PLCG2*, serve in a related pathway to allow microglia to respond to amyloid-β deposition, altered synaptic activity or damaged phospholipid membranes to activate phagocytosis via the complement system.[1,6,10,11] However, RNA-seq has also identified a parallel trajectory for activated microglia, distinct from DAM/ARM, the so-called 'interferon-response microglia' (IRM).[9,12–14] The number of IRM increases during normal ageing, and increases even further in response to amyloid pathology.[9,13] However, the mechanisms of action of IRM in both settings are not well understood.

Interferons (IFN) are cytokines that trigger a key response to mainly viral pathogens, and consist of three classes: type I (including IFN-α and IFN-β), type II (IFN-γ), and type III (IFN-λ). Interferon signalling is upregulated by an amplification loop in the presence of viruses such as influenza, hepatitis and severe acute respiratory syndrome coronavirus 2 (SARS-CoV-2), leading to the restriction of viral spread, by eliciting a number of molecular effectors to inhibit transcription of viral nucleic acids, digest viral RNA, block translation and modify protein function.[15] The microglial interferon response has recently been implicated in neuroinflammation and synapse loss in Alzheimer's disease; however, it is unclear how interferon signalling and antiviral immune response pathways in microglia contribute to Alzheimer's disease pathogenesis.[9,16–20] It has been proposed that nucleic acid-containing amyloid fibrils induce the expression of interferon-stimulated genes in Alzheimer's disease-associated mouse models, promoting the upregulation of pro-inflammatory markers and complement cascade-dependent synaptic elimination.[16,21] Another potential contributor to interferon signalling is the DNA-sensing receptor cyclic GMP–AMP synthase (cGAS) and its downstream mediator STimulator of INterferon Genes (STING; cGAS-STING pathway), which respond to not only pathogen-derived nucleic acids, but also mitochondrial and genomic nucleic acids derived from stressed, senescent or dying cells in the CNS.[22,23] While type I interferon signalling was reported to be associated with microglial activation patterns and Alzheimer's disease, there are implications that type II interferon signalling also contributes to neuroinflammation and Alzheimer's disease pathogenesis.[24–26]

The molecular machinery that drives antiviral responses includes interferon receptors (IFNAR and IFNGR), tyrosine kinase 2 (TYK2), IFN-stimulated protein of 15 kDa (ISG15, involved in an ubiquitin-like pathway), Mx GTPases (myxovirus resistance), protein kinase R (PKR; also known as eukaryotic translation initiation factor 2-alpha kinase 2, EIF2αK2), and the 2′,5′-oligoadenylate synthetase (OAS)-regulated ribonuclease L. Stimulation of interferon receptors leads to JAK-STAT signalling and induction of expression of interferon-stimulated genes, including *OAS1* from IFN-stimulated response elements (ISREs) in their promoters, resulting in the activation of RNase L, which in turn degrades cellular and viral RNA.[27,28] It has recently become apparent that the OAS proteins may also have additional functions that are independent of RNase L activity.[29–31] It has also been shown that *OAS1* is involved in the regulation of cytokine expression.[31] We recently identified *OAS1* as a putative new risk gene for Alzheimer's disease, by integrating DNA sequence variation at the gene-level from human genome-wide association studies (GWAS) associated with Alzheimer's disease, and a high-resolution RNA-seq transcriptome network expressed by mouse ARM.[12] The ARM transcriptome contains several genes involved in interferon signalling, including other mouse OAS genes, the interferon receptor *Ifnar2* and the coiled-coil alpha-helical rod protein 1, *Cchcr1*. In parallel work, recent GWAS have shown that several genes including *OAS1*, *IFNAR2* and *CCHCR1* involved in interferon signalling also contribute to the genetic risk associated with critical outcomes of coronavirus disease 2019 (COVID-19) and requirement for intensive care.[32,33] Deleterious gene variants have also been described in a number of genes involved in interferon signalling, including *IFNAR1*, *IFNAR2* and *IRF7* in patients with life-threatening COVID-19 pneumonia in an independent study.[34] Indeed, neutralizing autoantibodies against interferons have been identified in individuals with life-threatening COVID-19, where these antibodies dampen the interferon response.[35] These findings implicate the significance of interferon signalling pathways that could exacerbate the progression of Alzheimer's disease and the severity of COVID-19.

Similar to neurological manifestations caused by other respiratory viruses, including influenza virus and human respiratory syncytial virus,[36] the latest reports state that as many as 36–78% of individuals hospitalized with COVID-19 display neurological symptoms including encephalopathy, acute ischaemic cerebrovascular syndrome and neuropsychiatric manifestations.[37–40] Although it is controversial whether SARS-CoV-2 is detectable in the CSF, the virus uses angiotensin converting enzyme 2 (ACE2) as a key receptor for entry; ACE2 is expressed by the endothelium of

the blood–brain barrier, epithelial cells of the choroid plexus, and at a lower level by astrocytes, oligodendrocytes and nerve terminals (such as those of the olfactory system, which may allow retrograde spread).[41–45] There is accumulating evidence that these brain structures and cells are infected with SARS-CoV-2 and are altering the cytokine profile of the brain.[46,47] Elevated levels of pro-inflammatory cytokines including tumour necrosis factor-α (TNF-α), interleukin (IL)-1 and IL-6 in patients with severe COVID-19,[48–56] trigger an inflammatory cascade leading to cell death. Consequently, a blunted response by the interferon signalling pathway against pathogens implicates a higher risk for developing Alzheimer's disease and severe COVID-19. The ACE/ACE2 balance is disrupted in Alzheimer's disease, and it is common for individuals with hypertension and neurodegeneration to receive long-term treatment with ACE inhibitors and angiotensin II receptor blockers, which may ultimately increase ACE2 expression and so increase risk of infection with SARS-CoV-2 and disease severity.[57,58] Thus, the links between neurodegeneration, COVID-19, and neurological problems associated with COVID-19 are complex and likely involve multiple pathways. It is clear that investigating interferon pathways involved in antiviral responses will: (i) benefit our understanding of pathways involved in the progression of Alzheimer's disease and infectious diseases like COVID-19; and (ii) may provide new information for therapeutic approaches and identification of biomarkers to follow disease progression.

In this study, our genotyping analysis confirms that the single nucleotide polymorphism (SNP) rs1131454 within *OAS1* is significantly associated with Alzheimer's disease. We found that SNPs within *OAS1* associated with Alzheimer's disease also show linkage disequilibrium (LD) with SNP variants associated with critical illness in COVID-19. SNPs rs1131454 (risk allele A) and rs4766676 (risk allele T) are associated with Alzheimer's disease, and rs10735079 (risk allele A) and rs6489867 (risk allele T) are associated with critical illness with COVID-19, where these risk alleles show decreased expression of *OAS1*. Additionally, by investigating the transcriptome expressed by microglia and macrophages, we found genetic co-expression networks consisting of genes in interferon response pathways including *OAS1*, and the mouse orthologue *Oas1a*. In mouse microglia, the expression of this network was elevated with age and amyloid-β pathology. The equivalent co-expression network was also expressed in microglia from humans with Alzheimer's disease and mild cognitive impairment, and in bronchoalveolar lavage fluid (BALF) macrophages, where the expression of this network is elevated with severe COVID-19. Finally, we found that reducing the expression of *OAS1* using small interfering (si)RNA in human induced pluripotent stem cells (iPSCs) differentiated to microglia, results in an exaggerated pro-inflammatory response when stimulated with IFN-γ. Understanding the mechanisms by which *OAS1* pathways bridge interferon and pro-inflammatory signalling in innate immune cells will be important to gain new insights into the progression of Alzheimer's disease and severe/critical outcomes associated with COVID-19, and how to treat and track these diseases.

Materials and methods

Genotyping

DNA samples ($n = 2547$) were kindly obtained from six research institutes in the UK that are part of the Alzheimer's Research UK (ARUK) Network. The ARUK series of samples included here are from Bristol, Leeds, Manchester, Nottingham, Oxford and Southampton (further details are given in Appendix 1 and the Supplementary material). This ARUK series has not been included in the IGAP consortium study and consisted of confirmed or probable Alzheimer's disease diagnosis ($n = 1313$) and controls ($n = 1234$). Demographics for these samples are in Table 1. Since all demographic variables were found to be significantly different between the cases and controls ($P < 0.0001$), they were included as covariates in the subsequent analyses. The effects of covariates between cases and controls were tested for age (using a Student's *t*-test), and *APOE* status and sex (using chi-squared tests). Samples were genotyped in-house using a TaqMan® genotyping assay for rs1131454 following standard protocols (Applied Biosystems); the genotyping rate for the samples was 69.7%. Association of the SNP with Alzheimer's disease was conducted using logistic regression correcting for the covariates with the statistical analysis program PLINK.[59]

SNPs in the locus containing *OAS1* associated with Alzheimer's disease,[12,60] and COVID-19,[32] were illustrated with LocusZoom.[61] Allele frequencies and LD between these SNPs were investigated using the 1000Genomes Phase 3 data (European populations, CEU and GBR),[62] and LDlink,[63,64] where the LD between SNPs was calculated with the LDpair tool (available at https://ldlink.nci.nih.gov/?tab=ldpair using data from European populations, CEU, TSI and GBR). Allele-dependent expression of *OAS1* at the four SNPs of interest (rs1131454 and rs4766676 associated with Alzheimer's disease; rs10735079 and rs6489867 associated with critical illness with COVID-19), were investigated by mining data for whole blood, frontal cortex (BA9), and lung from the Genotype-Tissue Expression (GTEx) Project via the GTEx Portal on 17 June 2021.[65]

RNA-sequencing data preprocessing

The scRNA-seq datasets were generated from: (i) microglia isolated from the hippocampi of 3, 6, 12, and 21-month-old $APP^{NL\text{-}G\text{-}F}$ and wild-type mice (Sala Frigerio *et al.*,[9] denoted SF data; downloaded from GSE127893; non-hippocampal samples were removed); (ii) microglia isolated from the dorsolateral prefrontal cortex of human individuals with Alzheimer's disease or mild cognitive impairment (downloaded from Olah *et al.*,[19] denoted OL data; epilepsy samples and clusters of cells identified by the authors to express high levels of non-microglial or dissociation-induced genes were removed); and (iii) macrophages isolated from BALF of three patients with moderate COVID-19, six patients with severe/critical COVID-19, and three healthy controls (Liao *et al.*,[66] denoted LI data; downloaded from GSE145926). Datasets were filtered to remove cells that appeared either unhealthy (>5% ratio of mitochondrial to total counts for all datasets; <30 000 counts or <1000 genes detected for SF data; <1000 counts or <700 genes detected for OL data; <1000 counts or <200 genes for LI data), or potential doublets (>1 000 000 counts for SF data; >100 000 counts for OL data; >15 000 counts for LI data) using Seurat's subset function.[67] Counts were normalized using Seurat's *SCTransform* function with the method set to *glmGamPoi*, returning corrected Pearson's residuals.[68] The SF and OL data batch effects (sequencing plates for SF, patients for OL), were regressed out with *SCTransform*'s vars.to.regress argument. For LI data, because of significant inter-individual differences, cells from different patients were integrated using Seurat's reciprocal PCA integration workflow, with default settings, other than integrating all genes. Principal components were then calculated for the LI data, using Seurat's *RunPCA* function. Cells from the LI dataset were then clustered using Seurat's *FindNeighbours and FindClusters* functions, considering 30 principal components, and using the smart local moving algorithm at resolution 0.2. Clusters expressing *CD68* (macrophage marker), but not *FCGR3A* (monocyte marker), were considered to contain macrophages, and cells from all other clusters were removed. LI data

Table 1 SNP rs1131454 within *OAS1* is associated with Alzheimer's disease

	Mean AAD* (SD)	% Female*	% APOE* ε4 +	G-allele frequency	OR G-allele	P-value**
Alzheimer's disease (n = 1313)	76.7 (20.3)	60.9	59.9	0.407	0.82	0.0082
Control (n = 1234)	72.6 (11.4)	53.0	26.3	0.448		

Sample demographic and association result for the genotyping carried out on SNP rs1131454 within the *OAS1* gene using the IGAP independent samples from the ARUK DNA bank.

*Covariates for Alzheimer's disease including age at death (AAD), sex and presence of *APOE* ε4 alleles were found to be significantly different between cases and controls ($P < 0.0001$).

**The association of the G allele for a protective effect was significant after controlling for covariates.

were then reclustered as above. Raw counts and corrected Pearson's residuals were extracted from SF/OL data's Seurat objects, and raw counts and corrected and integrated Pearson's residuals were extracted from LI data's Seurat object. Genes not reliably detected (zero raw counts in >95% of cells in every cluster of cells, assigned by the original authors for SF/OL, or identified as above for LI data), were removed from all datasets. Finally, genes showing low variation in expression between cells (coefficient of variation for Pearson's residuals <15%) were removed, as they are not informative for co-expression analysis.

Bulk RNA-seq datasets generated from microglia isolated from the hippocampi of aged (22 months of age) and adult (2 months of age) wild-type mice,[69] the cortices of wild-type and *PSEN2/APP* mice at 14–15 months of age (PS2APP line),[13] or the parietal cortices of humans of different ages[70] were downloaded from GSE123847, GSE89482, and GSE99074, respectively. Data were normalized using DeSeq2's *estimatesizefactors* function and transformed by log2(normalized counts + 1).[71] Genes with an average detection level <1.5 normalized counts were removed. Expression associated with sequencing batch in the O'Neil *et al.*[69] dataset was removed using Limma's *RemoveBatchEffect* function, preserving the effect of age using the mod argument.[72] Batch information was not available for data from Friedman *et al.*,[13] or Galatro *et al.*[70]

Co-expression network analysis

Co-expression analysis was performed on preprocessed Pearson's residuals derived from scRNA-seq datasets using CoExpNets' *getDownstreamNetwork* function. CoExpNets is an optimization of the popular weighted gene co-expression network analysis (WGCNA) package,[73] which uses an additional k-means clustering step to reassign genes to more appropriate modules, producing more biologically relevant and reproducible modules.[74] The expression of the mouse interferon-response module was represented by the mean log2 normalized expression of the 60 most central module genes in microglia isolated from aged versus young adult wild-type mice, and *PSEN2/APP* versus wild-type mice, and by applying Student's *t*-test (the 60 most central module genes were ranked by module membership scores calculated by CoExpNets' *getMM* function) per sample in processed O'Neil *et al.*[69] and Friedman *et al.*[13] datasets, respectively. Linear regression was used to assess the association between the mean log2(normalized expression + 1) of the 60 most central module genes (as a proxy of module expression) and age in the human cortical microglia dataset,[70] accounting for the covariates of gender, site of origin, and post-mortem delay, using the R *lm* function. Two samples for which post-mortem delay was not provided, were not included in the regression. The assumptions of normality of residuals, homoscedasticity, and linearity were met, and the results were robust to removal of potential outliers. To assess the expression of the *OAS1*-containing module identified in LI data, we calculated the mean module eigengene score (first principal component of module expression, giving a reliable indicator of relative module expression in each cell) for macrophages from each patient. We assessed whether the mean module eigengene value was significantly influenced by COVID-19 status (healthy control, severe, and modest) using a Kruskal-Wallis test. Following a significant Kruskal-Wallis result ($P < 0.05$), group comparisons between control and modest disease, and control and severe disease were made with Dunn's multiple comparisons tests. Gene set enrichment analysis of genes present in both human *OAS1*-containing modules was conducted with the gprofiler2 R package,[75] using all the genes present in the co-expression analysis as a custom background, multiple test comparisons were accounted for by calculating an FDR using the Benjamini-Hochberg procedure.

Pseudotime analysis

To infer pseudotime trajectories of microglial activation, we followed the standard workflow of the Monocle 2 R package,[76,77] to calculate single-cell trajectories by ordering cells by their expression of the 1000 genes most significantly differentially expressed between cell clusters (ranked by qvalue), previously identified by Sala Frigerio *et al.*[9]

Cell culture

Human iPSC-derived microglia cells were generated from the BIONi010-C human iPSC line (EBiSC), originating from a non-demented, normal male (15–19 years old). Differentiation to human iPSC-derived microglia was essentially as described by Xiang *et al.*[78] Briefly, the protocol was as follows: embryoid body differentiation media for 2 days (consisted of Essential 8™, 50 ng/ml BMP4, 50 ng/ml VEGF, 20 ng/ml SCF, and 10 μM Y-27632), then myeloid differentiation media for 30 days [consisted of X-VIVO™ 15 medium (Lonza), GlutaMAX™ (Life Technologies), 100 U/ml penicillin/streptomycin (Life Technologies), 50 μM β-mercaptoethanol (Life Technologies), 100 ng/ml MCSF (Peprotech), and 25 ng/ml IL-3 (Cell Guidance Systems)]. These myeloid cells were seeded at a density of 5×10^5 cells/well in six-well plates, followed by microglial differentiation media for 13 days [consisted of: DMEM/F12 HEPES no phenol red, 2% ITS-G (Life Technologies), 1% N2 supplement (Life Technologies), 200 μM monothioglycerol (Sigma), GlutaMAX™, NEAA (Life Technologies), 5 μg/ml insulin (Sigma), 100 ng/ml IL-34 (Peprotech), 25 ng/ml MCSF and 5 ng/ml TGFβ-1 (Peprotech)] and finally, microglia maturation media for 4 days [consisted of: microglial differentiation media plus 100 ng/ml CD200 (Generon), and 100 ng/ml CX3CL1 (Peprotech)].

Small interfering RNA transfection

Human iPSC-derived microglia in six-well plates were treated with 125 μl Opti-MEM® containing 3.75 μl Lipofectamine® RNAiMAX (#13778150, Thermo Fisher Scientific), according to the

manufacturer's instructions, with 12.5 pmol of either non-targeting negative control siRNA showing no homology to the human transcriptome (#4457287, Ambion), or two different siRNAs targeting *OAS1* (siRNA-1 or -2, Ambion). The siRNA-1 and -2 were selected with an efficiency of 70–95% for *OAS1* knockdown in human iPSC-derived microglia. *OAS1* siRNA-1: sense 5′ GUCAA GCACUGGUACCAAAtt 3′, anti-sense 5′ UUUGGUACCAGUGCUUGA Cta 3′. *OAS1* siRNA-2: sense 5′ CCACUUUUCAGGAUCAGUUtt 3′, anti-sense 5′ AACUGAUCCUGAAAAGUGGtg 3′. Human iPSC-derived microglia were transfected 4 days after the switch to microglial maturation media. Cells were harvested for RNA extraction 24 1 h after transfection.

Interferon-γ treatment

Human iPSC-derived microglia were treated with 33 ng/ml human IFN-γ (#AF-300–02, PeproTech), at 4 h following siRNA transfection.

RNA extraction and cDNA synthesis

Prior to lysis, human iPSC-derived microglia cells were washed with Dulbecco's phosphate-buffered saline (DPBS). Total RNA was extracted using the Monarch Total RNA Miniprep Kit (#T2010S, NEB), following the manufacturer's guidelines. The total RNA quantity and purity (A_{260}/A_{280} ratio) were assessed with a NanoDrop spectrophotometer (Thermo Fisher Scientific). For further reduction of contaminating genomic DNA, equal amounts of RNA were treated with DNase I amplification grade (#18068015, Thermo Fisher Scientific) and RNaseOUT recombinant ribonuclease inhibitor (#10777019, Thermo Fisher Scientific). All RNA samples were reverse transcribed using the LunaScript™ RT supermix kit (#E3010L, NEB), according to the manufacturer's protocol. In parallel, negative controls were generated with the same procedure except the reverse transcriptase was omitted from the master mix (RT-negative control).

Real-time quantitative PCR

Primers for genes of interest were designed using Primer-BLAST (NCBI) to test their specificity against the whole human transcriptome. Primers were tested in two steps. The first step was to resolve the products of a standard PCR on a 3% agarose Tris-acetate-EDTA gel, stained with SYBR™ Safe (Thermo Fisher Scientific) to assess the correct product size and presence of only one product. The second step was to test the primers with RT-qPCR using SYBR™ Green to check the linearity range of a dilution series of cDNA template, to test primer efficiency (90–105%), and to confirm primer specificity using a melt curve. Primers with good efficiency were selected (Supplementary Table 1).

Each real-time quantitative PCR (RT-qPCR) reaction comprised 1.5 µl of cDNA, 0.25 µM forward and reverse primers, 5 µl of Luna® Universal qPCR Master Mix (#M3003L, NEB), and 3 µl of nuclease-free water. The reactions of each sample across the different conditions were loaded in triplicate with a RT-negative control sample. The reactions were run in 384-well plates on a LightCycler® 480 real-time PCR system (Roche) with cycling conditions of 95°C for 5 min (preincubation), 45 cycles of 95°C for 10 s, 60°C for 30 s (amplification), 95°C for 5 s, 65°C for 1 min, raised to 97°C (ramp rate 0.11°C/s) (melting curve). The product specificity of all reactions was confirmed by the melting curve analysis, where samples gave only a single peak and RT-negative control samples gave no signal. For normalization of gene expression levels, the stability of internal control reference genes was tested to ensure the reference genes used were stable across siRNA and IFN-γ treatment. The highest stability was seen with the geometric mean of Ct values of *RPS18*, *GAPDH*, and *HPRT1*. Gene expression analyses were performed by following the GeNorm method.[79,80]

ELISA of TNF-α secreted by human induced pluripotent stem cell-derived microglia

For ELISA analyses, supernatants from human iPSC-derived microglia cultures were collected, centrifuged to remove cell debris and stored at –20°C. TNF-α levels were quantified using the Quantikine human TNF-α ELISA kit (DTA00D, R&D Systems), following the manufacturer's instructions. In general, equal volumes of cell supernatants, together with the provided buffer, were loaded in duplicates to the ELISA microplate and incubated for 2 h. Following four washes, wells were then incubated with horseradish peroxidase conjugated human TNF-α antibody for another 2 h. The microplate was washed again and incubated with a substrate solution prepared with chromogen (TMB) and hydrogen peroxide for 30 min before addition of a stop solution with sulphuric acid. Then the colour intensity was measured at 450 nm, and 540 nm to assess the background signal, using a FLUOstar Omega microplate reader and the TNF-α concentrations in human iPSC-derived microglia supernatants were calculated from the standard curve.

Statistical analyses for cell culture experiments

All statistical analyses were conducted on GraphPad Prism 9. For experiments with human iPSC-derived microglia under basal conditions, comparisons between multiple groups were analysed by using repeated-measures one-way ANOVA (repeated for wells treated with different siRNA in the same plate) followed by Dunnett's multiple comparisons tests comparing every test group with the negative control group. For experiments with human iPSC-derived microglia in response to IFN-γ treatment and siRNA treatments, comparisons between factors were tested with two-way ANOVA followed with Tukey's multiple comparisons tests to compare all possible permutations of sample groups. Significant differences are indicated as follows: $^{*}P < 0.05$, $^{**}P < 0.01$, $^{***}P < 0.001$, $^{****}P < 0.0001$. Data are shown as mean standard error of the mean (SEM), where the sample size (n) represents individual cell preparations.

Data availability

The data that support the findings of this study are available from the corresponding author, upon reasonable request.

Results

SNPs associated with *OAS1* are linked to risk for Alzheimer's disease and critical illness with COVID-19

Our recent work overlapping the mouse amyloid-associated transcriptome network (bulk RNA-seq) with human gene-level-aggregated Alzheimer's disease risk variants, identified a microglial co-expression network, whose eigengene strongly correlated with the level of amyloid-β pathology and contained the mouse orthologues of many known human GWAS loci (including *TREM2 and APOE*).[12] This work also predicted the importance of several previously unidentified risk genes, including *OAS1*, and demonstrated a co-localization between Alzheimer's disease risk loci and expression quantitative trait loci (eQTLs) regulating *OAS1* expression in: (i) human iPSC-derived macrophages stimulated with a combination of IFN-γ and salmonella; and (ii) human monocytes stimulated with lipopolysaccharide or 5′-triphosphate dsRNA.[12,81,82]

To evaluate Alzheimer's disease-associated genetic variation in *OAS1*, we genotyped the top SNP, rs1131454, identified by our gene-level analysis of the Lambert *et al.*[83] GWAS. SNP rs1131454 was genotyped in 1313 individuals with sporadic Alzheimer's disease and 1234 control individuals that were not included in the original cohort from Lambert *et al.*[83] We found a significant association of rs1131454 with Alzheimer's disease in this independent cohort of Alzheimer's disease and control individuals (Table 1).

To determine whether Alzheimer's disease-associated SNPs in close proximity to *OAS1* were in LD with recently identified SNPs related to critical outcomes with COVID-19,[32] we used the 1000Genomes Phase 3 database (CEU and GBR populations)[62] (Fig. 1 and Table 2). Critical illness with COVID-19 was as defined by Pairo-Castineira *et al.*,[32] with a confirmed positive COVID-19 test result, and the treating clinician deemed the patient required continuous cardiorespiratory monitoring in an intensive care unit. We saw a strong LD (r^2 = 0.63–0.99 and D′ = 0.91–1.0) between our two top SNPs adjacent to *OAS1*, rs1131454 (identified using data from Lambert *et al.*[83]) and rs4766676 (identified using data from Kunkle *et al.*[84]), and two SNPs associated with severe COVID-19 responses, rs6489867 and rs10735079[32] using LDpair. This suggests that four risk alleles adjacent to the *OAS1* and *OAS3* genes may form part of a haplotype that contributes to both risk for Alzheimer's disease and a severe response with COVID-19 (Table 2). The risk alleles at each of the four SNPs we highlighted were associated with decreased expression of *OAS1* by mining the data from the GTEx Project[65] (Supplementary Fig. 1 and Supplementary Table 2). Significant effects were seen for all four SNPs associated with *OAS1* expression in whole blood, and while not significant for some SNPs, the same pattern was seen for frontal cortex and lung (where the contribution of myeloid cells to the signal is diluted by other cell types). In parallel, mining our transcriptome-wide association study (TWAS) analysis of Alzheimer's disease,[85] provided further evidence that genetic variants associated with decreased expression of *OAS1* are significantly more prevalent in patients with Alzheimer's disease (Supplementary Table 3). Together with results from our previous Alzheimer's disease-associated co-localization analyses,[12] the SNP-associated expression data in healthy individuals and patients with Alzheimer's disease presented here, suggests that there may be multiple complex or pleiotropic variant(s) within the *OAS* gene cluster that modulate risk for both Alzheimer's disease and severe COVID-19, via regulation of *OAS1* expression.[12,32,33]

Genetic networks involving *OAS1* are upregulated with ageing, amyloid plaques and severe COVID-19

To understand the microglial function of *OAS1*, we initially assessed the mouse orthologue, *Oas1a*, within co-expression networks generated from microglia isolated from $APP^{NL\text{-}G\text{-}F}$ knock-in and wild-type C57BL/6J mice at 3 to 21 months of age, profiled by scRNA-seq.[9] We identified a co-expression transcriptomic network containing *Oas1a* by utilizing a modified version of WGCNA, which produces more biologically relevant co-expression networks (Fig. 2A). The module containing *Oas1a* contained many interferon-responsive genes (*Ifit1*, *Ifit2*, *Ifit3*, *Ifitm3*, *Stat1*, *Stat2*, *Usp18* and *Mx1*), as expected, and pro-inflammatory cytokines (*Tnf*) (Supplementary Table 4). We then used semi-supervised pseudotime analysis to visualize how the expression of this gene module changes as microglia transition from a homeostatic state to two different activation states ARM and IRM (Fig. 2B). This revealed that *Oas1a* and the interferon-response module were upregulated in microglia that transition along one branch of this trajectory towards the IRM state (Fig. 2C). This module showed increased expression in microglia isolated and pooled (bulk RNA-seq) from aged wild-type mice compared with young mice (Fig. 2D). Moreover, this interferon module showed increased expression in microglial isolated and pooled from *PSEN2/APP* mice, which exhibit amyloid-β pathology characteristic of Alzheimer's disease, relative to wild-type mice (Fig. 2E). Importantly, performing similar analyses in microglia isolated from human brains with Alzheimer's disease,[19] we identified a related interferon-response network containing *OAS1* and other interferon-responsive genes (overlap with mouse IRM network $P = 3.7 \times 10^{-13}$, Fisher's exact test) (Fig. 3A and Supplementary Table 5). This human interferon-response module showed a significant positive association with age

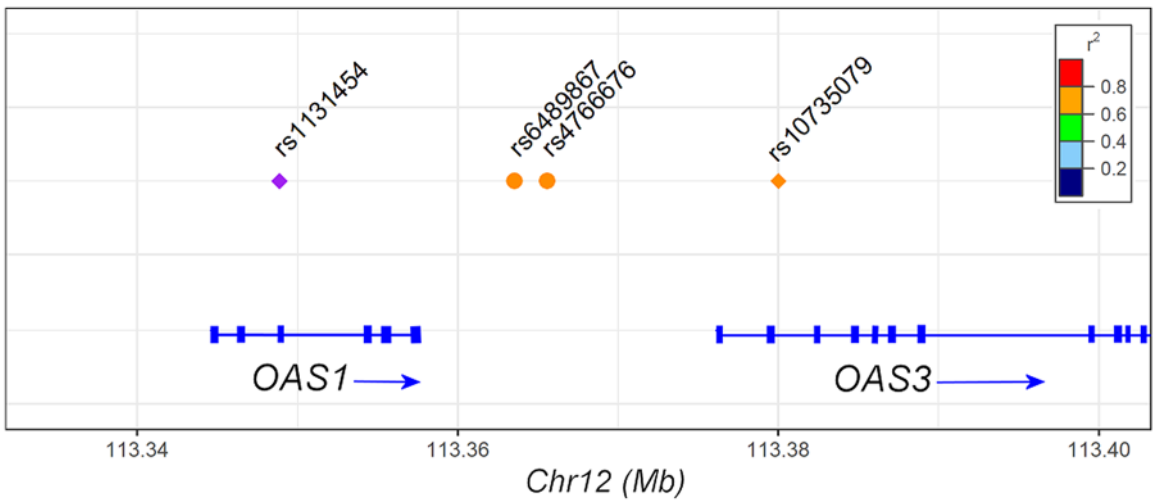

Figure 1 The genomic position of four SNPs on 12q24: rs1131454 and rs4766676 (associated with Alzheimer's disease) and rs10735079 and rs6489867 (associated with critical illness with COVID-19) relative to *OAS1*. We have confirmed rs1131454 is associated with Alzheimer's disease (Table 1) following our analysis of Alzheimer's disease GWAS data (our data is given in Salih *et al.*,[60] which was derived from further analysis of the GWAS data in Lambert *et al.*[83]). We identified the association of rs4766676 with Alzheimer's disease (our data is given in Salih *et al.*,[12] which was derived from further analysis of the GWAS data in Kunkle *et al.*[84]). SNPs rs10735079 and rs6489867 are associated with severe illness with COVID-19.[32] The R^2 scale indicates LD between rs1131454 (the reference SNP, purple), compared with the other three SNPs. Drawn with LocusZoom.[61]

Table 2 The frequencies of SNPs associated with Alzheimer's disease and COVID-19

RS number	Position (GRCh37)	Allele frequencies	Haplotypes			
rs1131454	chr12:113348870	A = 0.582, G = 0.418	A	G	G	A
rs6489867	chr12:113363550	T = 0.624, C = 0.376	T	C	T	C
rs4766676	chr12:113365581	T = 0.626, C = 0.374	T	C	T	C
rs10735079	chr12:113380008	A = 0.632, G = 0.368	A	G	A	G
		Haplotype count	213	132	23	7
		Haplotype frequency	0.5605	0.3474	0.0605	0.0184

Strong correlation between the SNPs associated with Alzheimer's disease and COVID-19 suggesting they might form part of a haplotype group. Allele frequency at these SNPs was investigated using the 1000Genomes Phase 3 data (CEU and GBR populations),[62] and LDlink.[63,64]

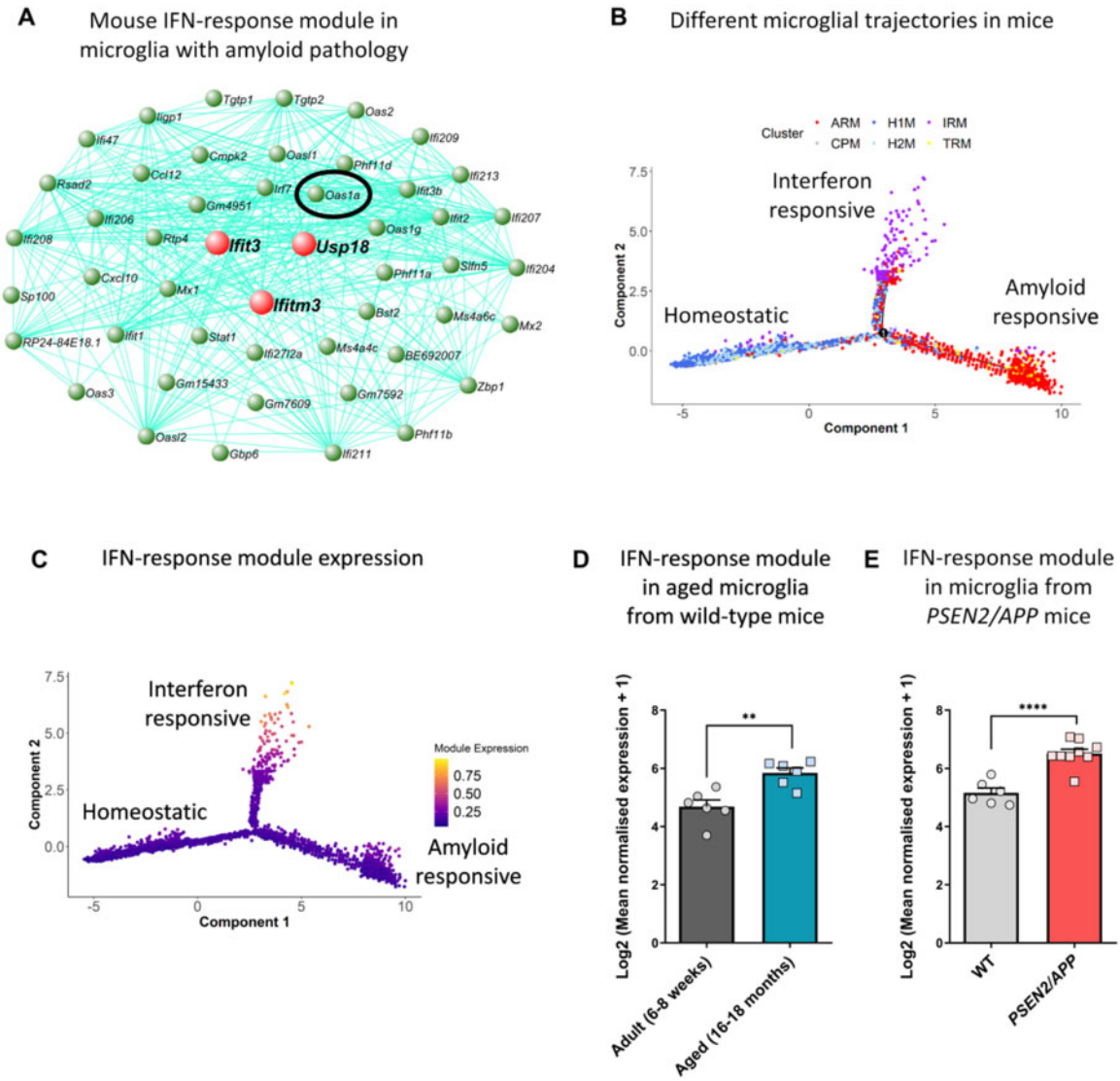

Figure 2 An interferon response-associated gene module is present along a distinct microglial activation trajectory upregulated in aged mice and mice with amyloid pathology. (**A**) The genetic network containing *Oas1a* from microglial cells isolated from wild-type and $APP^{NL\text{-}G\text{-}F}$ knock-in mice at 3, 6, 12 and 21 months of age analysed by scRNA-seq.[9] The 50 genes showing the highest connectivity are plotted, and *Oas1a* is highlighted with a black oval. Green nodes represent genes, edge lines represent co-expression connections, and the central large red nodes are the hub genes (the full network given in Supplementary Table 4). (**B**) Semi-supervised pseudotime ordering of microglial cells isolated from wild-type and $APP^{NL\text{-}G\text{-}F}$ knock-in mice based on expression,[9] with Monocle 2, shows homeostatic cells as the root state, and ARM and IRM as the end points of distinct activation trajectories. (**C**) The gene module containing *Oas1a* is upregulated (yellow data-points) along the IRM-associated activation trajectory. The expression of this module is relatively absent from both the root homeostatic state and the ARM trajectory (purple data-points). (**D**) Mean normalized expression of the 60 most central genes in the interferon-response module is greater in microglia isolated from aged wild-type relative to young adult mice (6–8 weeks versus 16–18 months of age; $n = 6$ mice per group). Data are shown as mean SEM. Student's *t*-test; $^{**}P < 0.01$. Further analysis of data from O'Neil *et al.*[69] (**E**) Mean normalized expression of the 60 most central genes in the interferon-response module is greater in microglia isolated from *PSEN2/APP* relative to wild-type mice at 14–15 months of age ($n = 6$–9 mice per group). Data are shown as mean SEM. Student's *t*-test; $^{****}P < 0.0001$. Further analysis of data from Friedman *et al.*[13]

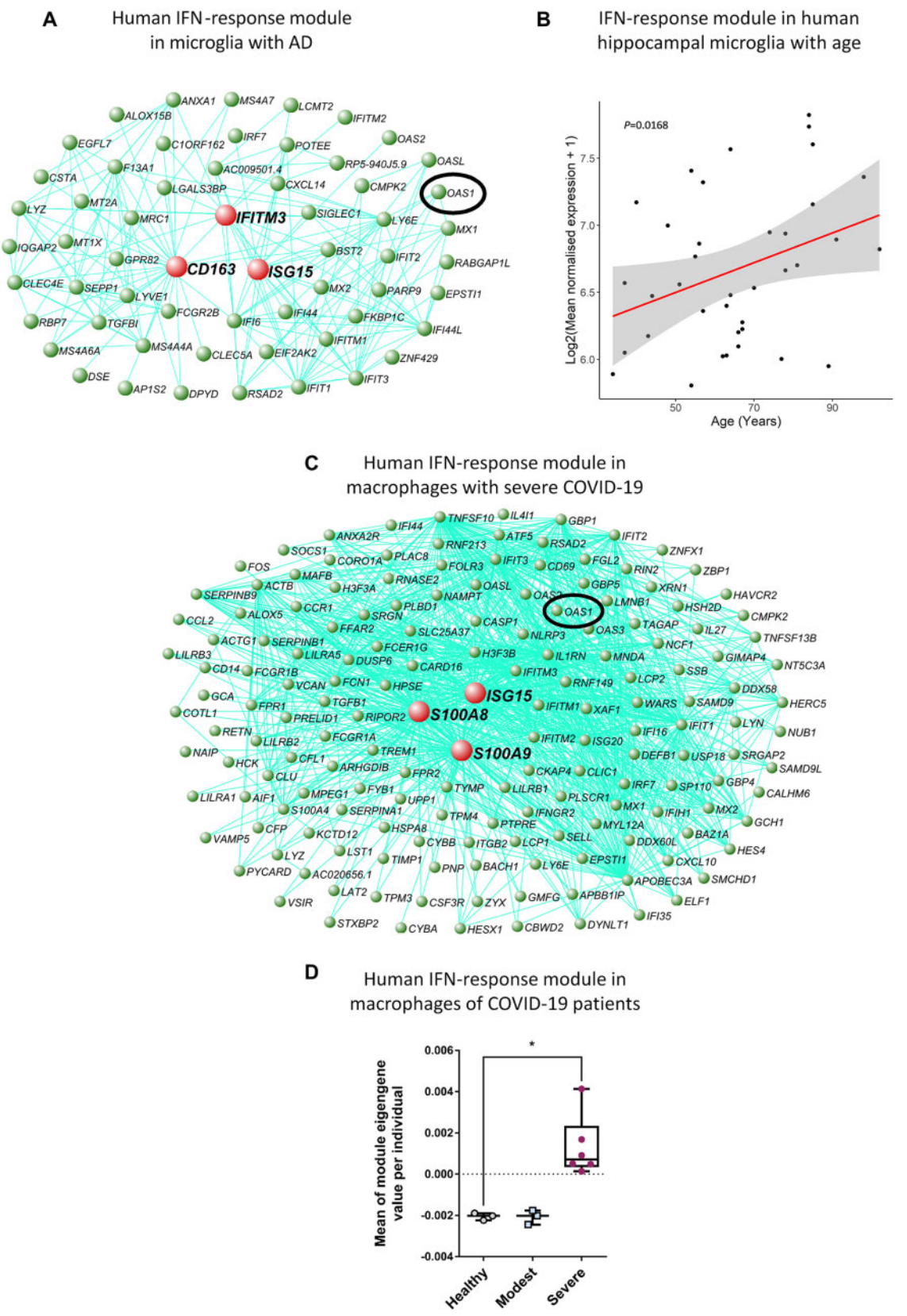

Figure 3 An interferon-response-associated gene module in the microglia of humans with Alzheimer's disease shows significant overlap with an interferon-response gene module in lung macrophages of patients with severe COVID-19. (**A**) Genetic network plot of an interferon-response associated module detected in microglial cells isolated from human Alzheimer's disease patients and individuals with MCI analysed by scRNA-seq.[19] This module shows a significant overlap with the interferon-response module detected in mice (Fig. 2A) (the full network is given in Supplementary Table 5). A hub gene of this module is *CD163*, and a number of other macrophage marker genes are prominent within this module (*TGFBI*, *F13A1*, *LY6E* and *LYZ*), indicating that expression of *OAS1* and other interferon-response genes in the human Alzheimer's disease patient brains are either associated

(Continued)

in microglia isolated and pooled from the parietal cortices of humans, ranging from 34 to 102 years of age,[70] even when factoring in the potential covariates of gender, site of origin, and post-mortem delay ($P = 0.0168$, coefficient = 0.016, linear regression) (Fig. 3B). These findings suggest that a discrete population of interferon-responsive microglia, defined by co-expression of *OAS1*, interferon-responsive genes, and pro-inflammatory cytokines, may play a role in amyloidosis, as well as ageing, the major risk factor for Alzheimer's disease and COVID-19.[86,87]

To investigate how the interferon-response microglial network containing *OAS1* from Alzheimer's disease brains was related to myeloid cell activation during COVID-19, we performed a similar analysis in BALF macrophages from COVID-19 patients with modest or severe disease, and healthy controls. We identified a co-expression module again containing *OAS1* and many interferon-responsive genes in BALF macrophages (Fig. 3C and Supplementary Table 6). This module partially overlapped with the microglial *OAS1*-containing module (64 genes common to both networks, $P = 7 \times 10^{-21}$, Fisher's exact test). Genes overlapping in the Alzheimer's disease microglial and COVID-19 macrophage networks showed significant enrichment for the 'type-I interferon response' GO term (FDR = 6.5×10^{-17}). The average expression of this module was elevated in macrophages from severe but not modest COVID-19 patients, relative to healthy controls ($P < 0.003$ for significant effect of disease state, Kruskal-Wallis test; mean module eigengene value in severe versus control $P = 0.031$, Dunn's multiple comparisons test) (Fig. 3D). These findings indicate that *OAS1* is expressed alongside interferon-responsive genes in alveolar macrophages, as well as microglia, and so may participate in the interferon-response in both myeloid subtypes. Furthermore, this response appears to be upregulated during severe COVID-19, ageing and amyloid-β pathology.

OAS1 coordinates the pro-inflammatory response of human induced pluripotent stem cell-derived microglia

To study the function of *OAS1* in human microglia, we used siRNA to knockdown expression of *OAS1* in human iPSC-derived microglia. We obtained knockdown of *OAS1* expression to around 30–40% of endogenous levels under non-stimulated conditions (Supplementary Fig. 2). Under these basal conditions, the expression profiles of commonly used markers covering various microglial functions including homeostasis, phagocytosis, pro- and anti-inflammatory signalling, and genes from the interferon-responsive networks, generally remained unchanged by *OAS1* knockdown in human iPSC-derived microglia. In response to IFN-γ treatment, *OAS1* expression increased by around 3.5-fold, and *OAS1* knockdown with siRNA was still effective in the presence of IFN-γ (Fig. 4A). Treatment with IFN-γ also induced the expression of pro-inflammatory marker *TNF* by around 30-fold in human iPSC-derived microglia, but with *OAS1* knockdown the induction of *TNF* was further significantly increased to around 45-fold compared with control cells treated with non-targeting siRNA (Fig. 4B). We confirmed the increased secretion of TNF-α into the human iPSC-derived microglia culture media in samples with *OAS1* knockdown in the presence of IFN-γ compared with cells treated with non-targeting siRNA and IFN-γ (Fig. 4C). At the same time, *C1QA* expression showed a significant but modest increase with *OAS1* knockdown (Fig. 4D). Treatment with IFN-γ resulted in increased expression of *TGFB1*, *CD68*, *P2RY12*, *IFITM3* and *STAT1*, decreased expression of *TREM2*, and had no effect on *IL1B*, *ITGAM* and *CD163* expression, with *OAS1* knockdown not altering the expression of these genes (Supplementary Fig. 3). Therefore, *OAS1* appeared to dampen the pro-inflammatory response involving TNF-α following IFN-γ stimulation, with a modest effect on dampening the expression of *C1QA* complement.

Discussion

GWAS studies have revealed the importance of innate immune cells in moderating the risk of Alzheimer's disease, with the discovery of variants in genes such as *TREM2*, *CD33* and *PLCG2*. A number of studies have shown that several of these genes are likely involved in the same signalling pathway or functioning in the same subpopulation of microglia to control their activation to a so-called DAM or ARM state.[8,9,88,89] These DAM or ARM cells are thought to regulate complement-dependent phagocytosis of synapses, which may be dependent on phospholipid signals presented on damaged cell membranes.[1,6,10,90,91] Emerging data also indicate that other subpopulations of microglia play a significant role in Alzheimer's disease and ageing, particularly the IRM cells, and may also express genes that confer risk for Alzheimer's disease.[9,12,13,19] We recently identified the interferon-responsive gene *OAS1* as a putative risk gene for Alzheimer's disease by combining transcriptional changes in the presence of amyloid plaques and gene-level variation from GWAS data.[12] Here, we confirm that rs1131454 within *OAS1* is associated with Alzheimer's disease when we genotype an independent cohort of 1313 individuals with Alzheimer's disease and 1234 control individuals. Additionally, we show that rs1131454 is in LD with newly identified SNPs associated with critical illness due to COVID-19, suggesting that the same locus regulates the risk for both Alzheimer's disease and severe outcomes with COVID-19. Furthermore, by building genetic transcriptome networks using scRNA-seq of isolated mouse microglia, we show that an interferon-response pathway containing the mouse orthologue *Oas1a* exhibits increased expression during ageing in microglia. This indicates that the expression of the

Figure 3 Continued
with a population of CNS border-associated or invading macrophages, or potentially a microglial subpopulation that upregulates anti-inflammatory genes. *OAS1* is highlighted with a black oval. (**B**) Linear regression of the mean normalized expression of the 60 most connected genes from the human interferon-response network in microglia isolated from the cortex of humans of different ages (range: 34–102 years of age) and profiled by RNA-seq by Galatro *et al.*[70] Linear regression formula: Log2(mean normalized expression + 1) = age + gender + site of origin + post-mortem delay. Data fulfils the assumptions of linearity, normality of residuals, and homoscedasticity, and shows no significant outliers. Red line depicts the line that minimizes distances to the observed values. Grey area depicts 95% confidence intervals. (**C**) Genetic network plot of an interferon-response-associated module detected in macrophages isolated from the bronchoalveolar fluid of patients with severe/critical and moderate COVID-19, alongside healthy individuals analysed by scRNA-seq.[66] This module shows a significant overlap with the interferon-response module detected in human Alzheimer's disease patients and individuals with MCI (Fig. 3A) (the full network given in Supplementary Table 6). A hub gene of this module is *ISG15*, and a number of other macrophage marker genes are prominent within this module (*TGFB1*, *LY6E* and *LYZ*). *OAS1* is highlighted with a black oval. (**D**) Expression of the *OAS1*-containing module in macrophages isolated from individuals with severe and modest COVID-19, alongside healthy controls. The mean module eigengene score was calculated as the first principal component of module expression, giving a reliable indicator of module expression for macrophages from each patient ($n = 6$ severe COVID-19 individuals, $n = 3$ modest COVID-19, and $n = 3$ healthy controls). Data are shown as a box-and-whisker plot, where the median is the box middle, the box is the interquartile range, and the whiskers are the minimum and maximum data-points. Kruskal-Wallis test showed a significant effect of disease status ($P < 0.01$). Dunn's multiple comparisons tests were then performed to test for pairwise significance between the healthy control and each COVID-19 group; *$P < 0.05$. Further analysis of data from Liao *et al.*[66]

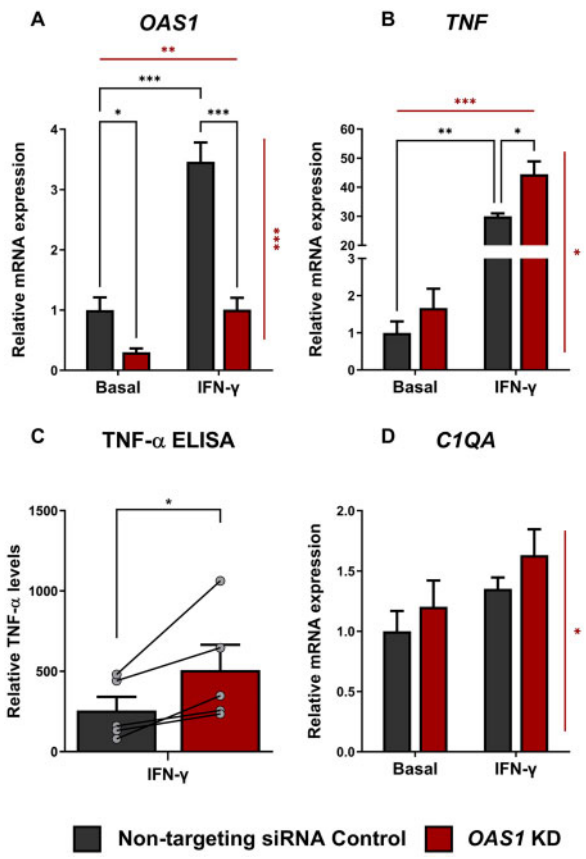

Figure 4 OAS1 knockdown in the presence of IFN-γ resulted in exaggerated expression of *TNF* in hman iPSCs differentiated to microglia. (**A**) *OAS1* expression was knocked-down using siRNA under basal conditions and in response to IFN-γ. Two-way ANOVA with significant main effects of IFN-γ treatment ($P < 0.01$), and siRNA treatment ($P < 0.001$) indicated as horizontal and vertical red lines, respectively, with a significant interaction ($P < 0.001$). (**B**) *TNF* expression, as a marker of the pro-inflammatory response, showed significant upregulation in response to IFN-γ application, and accentuated expression with *OAS1* knockdown. Two-way ANOVA with significant main effects of IFN-γ treatment ($P < 0.001$), and siRNA treatment ($P = 0.015$) indicated as horizontal and vertical red lines, respectively, with a significant interaction ($P = 0.023$). (**C**) ELISA of TNF-α levels in the conditioned human iPSC-derived microglia media. TNF-α levels were normalized to the geometric mean of *GAPDH*, *HPRT1* and *RPS18* assessed by RT-qPCR. Note that TNF-α protein was not detectable in the media of human iPSC-derived microglia not treated with IFN-γ. $n = 5$ independent plates. Data are shown as mean SEM. Paired Student's *t*-test (paired for wells on same plate); $^{*}P < 0.05$. (**D**) *C1QA* expression was increased with *OAS1* knockdown. Two-way ANOVA with significant main effect of only siRNA treatment ($P = 0.029$), not IFN-γ treatment ($P > 0.05$), indicated as a vertical red line, with no significant interaction ($P > 0.05$). Gene expression levels were normalized to the geometric mean of *GAPDH*, *HPRT1* and *RPS18*, then calculated as fold change relative to the non-targeting siRNA control (vehicle control) without IFN-γ treatment in each individual culture preparation. $n = 5$ independent plates. Data are shown as mean SEM. Two-way ANOVA; significant main effects of IFN-γ treatment and *OAS1*-knockdown indicated by red lines. When a significant interaction was seen between IFN-γ treatment and siRNA treatment, Tukey's multiple comparisons tests were then performed to test for pairwise significance of all groups; $^{*}P < 0.05$, $^{**}P < 0.01$, $^{***}P < 0.001$, $^{****}P < 0.0001$.

interferon pathway occurs within a specific subpopulation of innate immune cells and contributes to age-dependent changes that may predispose or protect some people in the population against these age-related diseases. We identify a related network of interferon-responsive genes containing *OAS1* in human microglia isolated post-mortem from patients with Alzheimer's disease, which also shows increased expression with age in microglia isolated from healthy individuals. Furthermore, macrophages from patients with severe COVID-19 upregulate an interferon-response-associated gene network containing *OAS1* that significantly overlaps with the Alzheimer's disease-associated microglial network. Finally, with functional experiments using human iPSC-derived microglia, we show that *OAS1* levels moderate the pro-inflammatory response of myeloid cells in response to elevated interferon levels. Thus, individuals with lower levels of *OAS1* due to eQTL variants may show a strong pro-inflammatory response to Alzheimer's disease-associated pathology and COVID-19, potentially triggering damage and cell death in neighbouring cells such as neurons and alveolar cells, by initiating a 'cytokine storm'.

The data presented here provide support for *OAS1* linking Alzheimer's disease and critical illness with COVID-19 by controlling the pro-inflammatory output of myeloid cells. OAS1 is an oligoadenylate synthetase enzyme that binds dsRNA and changes conformation to generate oligoadenylates and activate RNase L to digest RNA.[92,93] It has also been proposed that OAS1 may have RNase-independent roles.[29,30] *OAS1* is expressed by multiple cell types in the myeloid lineage including monocytes, macrophages, and microglia, as well as natural killer cell lymphocytes.[33,81,82,94] Here, we show that rs1131454 within *OAS1* is associated with Alzheimer's disease, and previously we showed that this locus acts as an eQTL regulating the expression of *OAS1* in monocytes and iPSC macrophages stimulated with 5′-triphosphate dsRNA and a combination of IFN-γ and salmonella, respectively.[12] Also in the same locus is *OAS2*, which was independently shown to be associated with Alzheimer's disease.[95,96] Recent work has identified other SNPs close to this locus associated with severe responses to COVID-19 that also act as eQTLs and regulate the expression of *OAS1*, *OAS3* and other distal genes such as *DTX1*.[32,33,97] Indeed, a series of different variants have been identified within *OAS1* that modify susceptibility to infection with SARS-CoV-2, other viruses such as hepatitis C, developing type 1 diabetes, and multiple sclerosis; these variants have been proposed to cause amino acid changes, altered splicing (spliceQTLs) and altered expression (eQTLs).[98–104] A recent study has identified a haplotype of ~75 kb centred around the *OAS* locus inherited from Neanderthals that is protective against COVID-19,[104] suggesting that there has been genetic selection at this locus during European history. Given the variety of SNPs associated with *OAS1* and their influence on diseases related to innate immune function, this suggests that these SNPs tag a complex and/or pleiotropic genetic variant that alters the expression of *OAS1*, as opposed to a variant that alters *OAS1* enzyme activity. The different SNPs tagging the *OAS1* variant may be in different chromosomal positions in different people, with different effect sizes. It is also possible that varying LD in individuals within different studies and populations results in the true causal variant being tagged by different SNPs in different people and studies. Several studies described here show altered expression of *OAS1* associated with these SNPs. Another possibility that has been proposed is that different SNPs within this locus differentially regulate the expression of genes within this cluster in different immune cells based on chromatin conformation,[33] although further work needs to be done to test the effects of different variants in other immune cell types including microglia and other tissue-specific macrophages, such as alveolar macrophages.

Lowering the expression of *OAS1* using siRNA to mimic the effects of an eQTL demonstrated that *OAS1* is required to dampen the expression and release of pro-inflammatory marker TNF-α when the levels of IFN-γ increase. Thus, individuals with eQTL variants that result in lower levels of *OAS1* expression may show more severe disease phenotypes associated with both Alzheimer's

disease and COVID-19, as a result of increased TNF-α and other pro-inflammatory cytokines. TNF-α and IFN-γ have been shown to have a synergistic effect on cell death,[54] and so could damage nearby neurons and alveolar cells. TNF-α with C1Q complement (which also shows elevated expression in our human iPSC-derived microglia system in response to *OAS1* knockdown), has been shown to induce the activation of reactive astrocytes, which contribute to synaptic damage, phagocytosis, and death of neurons and oligodendrocytes.[105] Previously, we and others have shown that pro-inflammatory signals also suppress the expression of *Trem2* via TLR4 receptors.[106–109] Our data are consistent with the suppression of *TREM2* expression as a response to IFN-γ and TNF-α in human iPSC-derived microglia. Given that TREM2 is likely to have a protective role in Alzheimer's disease and slow disease progression, elevated pro-inflammatory signals could increase the risk and progression of Alzheimer's disease by suppressing this protective signal. TNF-α also activates PKR/EIF2αK2, which is downstream of interferon signalling via TLR4, and consequently the protein activator of the IFN-inducible protein kinase (PRKRA) leading to apoptosis.[15,110] Altogether, chronic elevation of interferon signalling and subsequent TNF-α release could contribute to the development of dementia.

Pseudotime and network analysis of microglia isolated from $APP^{NL\text{-}G\text{-}F}$ and wild-type C57BL/6J mice across a variety of ages identified that *Oas1a* was upregulated alongside a co-expression network associated with interferon and pro-inflammatory responses expressed by a distinct sub-population of microglia transitioning to the IRM state. This network contained *Oas1a* (the mouse orthologue of *OAS1* with 68% identity at the protein level), other *Oas* family members, *Mx1*, *Stat1/2*, and *Ifit3*, *Ifitm3 and Usp18* as hub genes. The expression of this network of genes was increased with age in wild-type mice, and the equivalent human network was increased with age in microglia isolated from healthy humans. This finding suggests that the upregulation of interferon-responsive genes with age might mitigate the age-related damage by limiting pro-inflammatory signalling. Any dysfunction due to genetic variants in interferon signalling could result in persistent pro-inflammatory signalling and/or suppression of protective genes such as *TREM2*, which could lead to dementia or severe COVID-19. Age is one of the strongest risk factors for severe COVID-19 responses and Alzheimer's disease,[86,87] and so understanding the function of this genetic network will be important to attenuate the age-dependent contribution to these diseases.

The interferon-responsive genes seen in aged mice, and mice with amyloid plaques, were also expressed in a specific sub-population of microglia that are present in brains from people with Alzheimer's disease.[19] The genetic network we identified in human brains with Alzheimer's disease containing *OAS1* and other interferon-responsive genes, identified *IFITM3*, *CD163* and *ISG15* as hub genes. CD163 is a marker of a subset of border-associated macrophages (BAMs) that are present at the borders of the brain, including the meninges and choroid plexus, and is thought to represent an anti-inflammatory state in these cells, indicating the resolution of inflammation.[111–114] Indeed, emerging evidence suggests that SARS-CoV-2 is able to infect the brain vasculature, meninges and choroid plexus,[46] which would result in activation of BAMs and alter the cytokine environment around the brain leading to blood–brain barrier breakdown, infiltration of immune cells into the brain, activation of astrocytes and phagocytosis of neurons. Coupling these findings with the high incidence of neurological problems in people showing a severe COVID-19 response,[37–40] emphasizes the urgency with which we need to understand the mechanisms underlying the changes to cytokine signalling regulated by interferon signalling, particularly to anticipate the long-term neurological consequences of COVID-19.[115] In addition to COVID-19, a SNP within *OAS1* was also associated with type 1 diabetes and so *OAS1* may integrate multiple risk factors that contribute to critical outcomes with COVID-19.[99]

Surveying the genetic network we have identified containing *OAS1*, there are a number of secreted factors that may be useful as a readout of the state of these specialized innate immune cells in blood or CSF. The secreted genes include: *F13A1*, *ISG15* and *TNFSF13B*. The identification of *OAS1 and OAS3* as genes that coordinate the response to amyloid-β plaques and COVID-19 infection poses the use of phosphodiesterase 12 (PDE12) inhibitors to increase the activity of OAS enzymes for these diseases, since PDE12 degrades the oligoadenylate activator of the OAS/RNase L system.[116] PDE12 inhibitor compounds or *PDE12* knockout increase the anti-viral activity of cells. Furthermore, administration of interferons with correct timing may also help to dampen the pro-inflammatory response of innate immune cells, as in the treatment of multiple sclerosis.[52,117–119]

In conclusion, our data show that OAS1 is required to limit the pro-inflammatory response of myeloid cells when stimulated with IFN-γ. We also identify a SNP within *OAS1* associated with Alzheimer's disease in the same locus that predisposes to critical illness with COVID-19. This SNP acts as an eQTL, and is common in the population, and so may contribute to the high incidence of Alzheimer's disease or critical illness with COVID-19 in the population. Further investigation of the function of OAS1 in innate immune cells and the genetic network engaged by *OAS1* will provide better molecular targets to track disease progression and treat Alzheimer's disease, as well as COVID-19 and potentially its long-term sequelae.

Funding

N.M. was supported by Alzheimer Nederland, the Erasmus+ Traineeship programme, and then a PhD studentship funded by Eli Lilly and Co. T.M.P. was supported by funding to J.M.P. and J.H. from the Innovative Medicines Initiative 2 Joint Undertaking under grant agreement 115976. This Joint Undertaking receives support from the European Union's Horizon 2020 research and innovation programme and the European Federation of Pharmaceutical Industries and Associations (EFPIA). R.H.R. was supported through the award of a Leonard Wolfson Doctoral Training Fellowship in Neurodegeneration. J.A.B. is supported through the Science and Technology Agency, Séneca Foundation, CARM, Spain (research project 00007/COVI/20). The University of Nottingham Group is funded by ARUK and hosts the ARUK Consortium DNA Bank, with the members given in the Appendix below. J.H. is supported by the Dolby Foundation, and by the National Institute for Health Research University College London Hospitals Biomedical Research Centre. D.A.S. also received funding from the Alzheimer's Research UK (ARUK) pump priming scheme via the UCL network. This work was funded by the UK DRI, which receives its funding from the DRI Ltd, funded by the UK Medical Research Council, Alzheimer's Society and ARUK.

Competing interests

The authors report no competing interests.

Supplementary material

Supplementary material is available at *Brain* online.

Appendix I

Full details are provided in the Supplementary material.

The University of Nottingham Group is funded by ARUK and hosts the ARUK Consortium DNA Bank, with the members: Tulsi Patel, David M. Mann, Peter Passmore, David Craig, Janet Johnston, Bernadette McGuinness, Stephen Todd, Reinhard Heun, Heike Kölsch, Patrick G. Kehoe, Emma R. L. C. Vardy, Nigel M. Hooper, Stuart Pickering-Brown, Julie Snowden, Anna Richardson, Matt Jones, David Neary, Jenny Harris, A. David Smith, Gordon Wilcock, Donald Warden and Clive Holmes.

References

1. Edwards FA. A unifying hypothesis for Alzheimer's disease: From plaques to neurodegeneration. *Trends Neurosci*. 2019; 42(5):310–322.
2. Leyns CEG, Gratuze M, Narasimhan S, et al. TREM2 function impedes tau seeding in neuritic plaques. *Nat Neurosci*. 2019; 22(8):1217–1222.
3. Yuan P, Condello C, Keene CD, et al. TREM2 haplodeficiency in mice and humans impairs the microglia barrier function leading to decreased amyloid compaction and severe axonal dystrophy. *Neuron*. 2016;90(4):724–739.
4. Ising C, Venegas C, Zhang S, et al. NLRP3 inflammasome activation drives tau pathology. *Nature*. 2019;575(7784):669–673.
5. Efthymiou AG, Goate AM. Late onset Alzheimer's disease genetics implicates microglial pathways in disease risk. *Mol Neurodegener*. 2017;12(1):43.
6. Hardy J, Escott-Price V. Genes, pathways and risk prediction in Alzheimer's disease. *Hum Mol Genet*. 2019;28(R2):R235–240.
7. Sims R, van der Lee SJ, Naj AC, et al.; ARUK Consortium. Rare coding variants in PLCG2, ABI3, and TREM2 implicate microglial-mediated innate immunity in Alzheimer's disease. *Nat Genet*. 2017;49(9):1373–1384.
8. Keren-Shaul H, Spinrad A, Weiner A, et al. A unique microglia type associated with restricting development of Alzheimer's disease. *Cell*. 2017;169(7):1276–1290.e17.
9. Sala Frigerio C, Wolfs L, Fattorelli N, et al. The major risk factors for Alzheimer's disease: Age, sex, and genes modulate the microglia response to Aβ plaques. *Cell Rep*. 2019;27(4): 1293–1306.e6.
10. Hong S, Beja-Glasser VF, Nfonoyim BM, et al. Complement and microglia mediate early synapse loss in Alzheimer mouse models. *Science*. 2016;352(6286):712–716.
11. Parhizkar S, Arzberger T, Brendel M, et al. Loss of TREM2 function increases amyloid seeding but reduces plaque-associated ApoE. *Nat Neurosci*. 2019;22(2):191–204.
12. Salih DA, Bayram S, Guelfi S, et al. Genetic variability in response to amyloid beta deposition influences Alzheimer's disease risk. *Brain Commun*. 2019;1(1):fcz022.
13. Friedman BA, Srinivasan K, Ayalon G, et al. Diverse brain myeloid expression profiles reveal distinct microglial activation states and aspects of Alzheimer's disease not evident in mouse models. *Cell Rep*. 2018;22(3):832–847.
14. Ellwanger DC, Wang S, Brioschi S, et al. Prior activation state shapes the microglia response to antihuman TREM2 in a mouse model of Alzheimer's disease. *Proc Natl Acad Sci U S A*. 2021;118:e2017742118.
15. Sadler AJ, Williams BRG. Interferon-inducible antiviral effectors. *Nat Rev Immunol*. 2008;8(7):559–568.
16. Roy ER, Wang B, Wan Y, et al. Type I interferon response drives neuroinflammation and synapse loss in Alzheimer disease. *J Clin Invest*. 2020;130(4):1912–1930.
17. Heuer SE, Neuner SM, Hadad N, et al. Identifying the molecular systems that influence cognitive resilience to Alzheimer's disease in genetically diverse mice. *Learn Mem*. 2020;27(9): 355–371.
18. Mathys H, Davila-Velderrain J, Peng Z, et al. Single-cell transcriptomic analysis of Alzheimer's disease. *Nature*. 2019; 570(7761):332–337.
19. Olah M, Menon V, Habib N, et al. Single cell RNA sequencing of human microglia uncovers a subset associated with Alzheimer's disease. *Nat Commun*. 2020;11(1):6129.
20. Sebastian Monasor L, Müller SA, Colombo AV, et al. Fibrillar Aβ triggers microglial proteome alterations and dysfunction in Alzheimer mouse models. *Elife*. 2020;9:e54083.
21. Di Domizio J, Zhang R, Stagg LJ, et al. Binding with nucleic acids or glycosaminoglycans converts soluble protein oligomers to amyloid. *J Biol Chem*. 2012;287(1):736–747.
22. Motwani M, Pesiridis S, Fitzgerald KA. DNA sensing by the cGAS–STING pathway in health and disease. *Nat Rev Genet*. 2019;20(11):657–674.
23. Paul BD, Snyder SH, Bohr VA. Signaling by cGAS-STING in neurodegeneration, neuroinflammation, and aging. *Trends Neurosci*. 2021;44(2):83–96.
24. Deczkowska A, Baruch K, Schwartz M. Type I/II interferon balance in the regulation of brain physiology and pathology. *Trends Immunol*. 2016;37(3):181–192.
25. Majoros A, Platanitis E, Kernbauer-Hölzl E, Rosebrock F, Müller M, Decker T. Canonical and non-canonical aspects of JAK-STAT signaling: Lessons from interferons for cytokine responses. *Front Immunol*. 2017;8:29.
26. Taylor JM, Moore Z, Minter MR, Crack PJ. Type-I interferon pathway in neuroinflammation and neurodegeneration: Focus on Alzheimer's disease. *J Neural Transm*. 2018;125(5):797–807.
27. Silverman RH. Viral encounters with 2′,5′-oligoadenylate synthetase and RNase L during the interferon antiviral response. *J Virol*. 2007;81(23):12720–12729.
28. Donovan J, Dufner M, Korennykh A. Structural basis for cytosolic double-stranded RNA surveillance by human oligoadenylate synthetase 1. *Proc Natl Acad Sci U S A*. 2013;110(5): 1652–1657.
29. Kristiansen H, Scherer CA, McVean M, et al. Extracellular 2′-5′ oligoadenylate synthetase stimulates RNase L-independent antiviral activity: A novel mechanism of virus-induced innate immunity. *J Virol*. 2010;84(22):11898–11904.
30. Li Y, Banerjee S, Wang Y, et al. Activation of RNase L is dependent on OAS3 expression during infection with diverse human viruses. *Proc Natl Acad Sci U S A*. 2016;113(8):2241–2246.
31. Lee W-B, Choi WY, Lee D-H, Shim H, Kim-Ha J, Kim Y-J. OAS1 and OAS3 negatively regulate the expression of chemokines and interferon-responsive genes in human macrophages. *BMB Rep*. 2019;52(2):133–138.
32. Pairo-Castineira E, Clohisey S, Klaric L, et al.; Gen-COVID Investigators. Genetic mechanisms of critical illness in Covid-19. *Nature*. 2021;591(7848):92–98.
33. Schmiedel BJ, Chandra V, Rocha J, et al. COVID-19 genetic risk variants are associated with expression of multiple genes in diverse immune cell types. *bioRxiv*. [Preprint] doi:10.1101/2020.12.01.407429
34. Zhang Q, Bastard P, Liu Z, et al.; NIAID-USUHS/TAGC COVID Immunity Group. Inborn errors of type I IFN immunity in patients with life-threatening COVID-19. *Science*. 2020; 370(6515):eabd4570.
35. Bastard P, Rosen LB, Zhang Q, et al.; COVID Human Genetic Effort. Autoantibodies against type I IFNs in patients with life-threatening COVID-19. *Science*. 2020;370(6515):eabd4585.

36. Bohmwald K, Gálvez NMS, Ríos M, Kalergis AM. Neurologic alterations due to respiratory virus infections. *Front Cell Neurosci*. 2018;12:386.
37. Mao L, Jin H, Wang M, et al. Neurologic manifestations of hospitalized patients with coronavirus disease 2019 in Wuhan, China. *JAMA Neurol*. 2020;77(6):683–690.
38. Romero-Sánchez CM, Díaz-Maroto I, Fernández-Díaz E, et al. Neurologic manifestations in hospitalized patients with COVID-19. *Neurology*. 2020;95(8):e1060–e1070.
39. Woo MS, Malsy J, Pöttgen J, et al. Frequent neurocognitive deficits after recovery from mild COVID-19. *Brain Commun*. 2020; 2(2):fcaa205.
40. Paterson RW, Brown RL, Benjamin L, et al. The emerging spectrum of COVID-19 neurology: Clinical, radiological and laboratory findings. *Brain*. 2020;143(10):3104–3120.
41. Butowt R, von Bartheld CS. Anosmia in COVID-19: Underlying mechanisms and assessment of an olfactory route to brain infection. *Neuroscientist*. Published online 11 September 2020. doi:10.1177/1073858420956905
42. Desforges M, Le Coupanec A, Stodola JK, Meessen-Pinard M, Talbot PJ. Human coronaviruses: Viral and cellular factors involved in neuroinvasiveness and neuropathogenesis. *Virus Res*. 2014;194:145–158.
43. Paniz-Mondolfi A, Bryce C, Grimes Z, et al. Central nervous system involvement by severe acute respiratory syndrome coronavirus-2 (SARS-CoV-2). *J Med Virol*. 2020;92(7):699–702.
44. de Klein N, Tsai EA, Vochteloo M et al. Brain expression quantitative trait locus and network analysis reveals downstream effects and putative drivers for brain-related diseases. *bioRxiv*. [Preprint]. doi:10.1101/2021.03.01.433439
45. Chen R, Wang K, Yu J, et al. The spatial and cell-type distribution of SARS-CoV-2 receptor ACE2 in the human and mouse brains. *Front Neurol*. 2020;11:573095.
46. Yang AC, Kern F, Losada PM, et al. Dysregulation of brain and choroid plexus cell types in severe COVID-19. *Nature*. 2021; 595(7868):565–571.
47. Matschke J, Lütgehetmann M, Hagel C, et al. Neuropathology of patients with COVID-19 in Germany: A post-mortem case series. *Lancet Neurol*. 2020;19(11):919–929.
48. Chevrier S, Zurbuchen Y, Cervia C, et al. A distinct innate immune signature marks progression from mild to severe COVID-19. *Cell Reports Med*. 2021;2(1):100166.
49. Hadjadj J, Yatim N, Barnabei L, et al. Impaired type I interferon activity and inflammatory responses in severe COVID-19 patients. *Science*. 2020;369(6504):718–724.
50. Huang C, Wang Y, Li X, et al. Clinical features of patients infected with 2019 novel coronavirus in Wuhan, China. *Lancet*. 2020;395(10223):497–506.
51. Keddie S, Ziff O, Chou MKL, et al. Laboratory biomarkers associated with COVID-19 severity and management. *Clin Immunol*. 2020;221:108614.
52. Lee JS, Shin E-C. The type I interferon response in COVID-19: Implications for treatment. *Nat Rev Immunol*. 2020;20(10): 585–586.
53. Qin C, Zhou L, Hu Z, et al. Dysregulation of immune response in patients with coronavirus 2019 (COVID-19) in Wuhan, China. *Clin Infect Dis*. 2020;71(15):762–768.
54. Karki R, Sharma BR, Tuladhar S, et al. Synergism of TNF-α and IFN-γ triggers inflammatory cell death, tissue damage, and mortality in SARS-CoV-2 infection and cytokine shock syndromes. *Cell*. 2021;184(1):149–168.e17.
55. Chen G, Wu D, Guo W, et al. Clinical and immunological features of severe and moderate coronavirus disease 2019. *J Clin Invest*. 2020;130(5):2620–2629.
56. Lee JS, Park S, Jeong HW, et al. Immunophenotyping of COVID-19 and influenza highlights the role of type I interferons in development of severe COVID-19. *Sci Immunol*. 2020;5(49): eabd1554.
57. Haghighi MM, Kakhki EG, Sato C, Ghani M, Rogaeva E. The intersection between COVID-19, the gene family of ACE2 and Alzheimer's disease. *Neurosci Insights*. 2020;15: 2633105520975743.
58. Xia X, Wang Y, Zheng J. COVID-19 and Alzheimer's disease: How one crisis worsens the other. *Transl Neurodegener*. 2021; 10(1):15.
59. Purcell S, Neale B, Todd-Brown K, et al. PLINK: A tool set for whole-genome association and population-based linkage analyses. *Am J Hum Genet*. 2007;81(3):559–575.
60. Salih DA, Bayram S, Guelfi MS et al. Genetic variability in response to Aβ deposition influences Alzheimer's risk. *bioRxiv*. [Preprint] doi:10.1101/437657
61. Pruim RJ, Welch RP, Sanna S, et al. LocusZoom: Regional visualization of genome-wide association scan results. *Bioinformatics*. 2010;26(18):2336–2337.
62. Auton A, Brooks LD, Durbin RM, et al.; 1000 Genomes Project Consortium. A global reference for human genetic variation. *Nature*. 2015;526(7571):68–74.
63. Myers TA, Chanock SJ, Machiela MJ. LDlinkR: An R package for rapidly calculating linkage disequilibrium statistics in diverse populations. *Front Genet*. 2020;11:157.
64. Machiela MJ, Chanock SJ. LDlink: A web-based application for exploring population-specific haplotype structure and linking correlated alleles of possible functional variants. *Bioinformatics*. 2015;31(21):3555–3557.
65. GTEx Consortium. Human genomics. The Genotype-Tissue Expression (GTEx) pilot analysis: Multitissue gene regulation in humans. *Science*. 2015;348(6235):648–660.
66. Liao M, Liu Y, Yuan J, et al. Single-cell landscape of bronchoalveolar immune cells in patients with COVID-19. *Nat Med*. 2020; 26(6):842–844.
67. Stuart T, Butler A, Hoffman P, et al. Comprehensive integration of single-cell data. *Cell*. 2019;177(7):1888–1902.e21.
68. Hafemeister C, Satija R. Normalization and variance stabilization of single-cell RNA-seq data using regularized negative binomial regression. *Genome Biol*. 2019;20(1):296-
69. O'Neil SM, Witcher KG, McKim DB, Godbout JP. Forced turnover of aged microglia induces an intermediate phenotype but does not rebalance CNS environmental cues driving priming to immune challenge. *Acta Neuropathol Commun*. 2018;6(1):129.
70. Galatro TF, Holtman IR, Lerario AM, et al. Transcriptomic analysis of purified human cortical microglia reveals age-associated changes. *Nat Neurosci*. 2017;20(8):1162–1171.
71. Love MI, Huber W, Anders S. Moderated estimation of fold change and dispersion for RNA-seq data with DESeq2. *Genome Biol*. 2014;15(12):550.
72. Ritchie ME, Phipson B, Wu D, et al. Limma powers differential expression analyses for RNA-sequencing and microarray studies. *Nucleic Acids Res*. 2015;43(7):e47.
73. Langfelder P, Horvath S. WGCNA: An R package for weighted correlation network analysis. *BMC Bioinformatics*. 2008;9:559.
74. Botía JA, Vandrovcova J, Forabosco P, et al.; United Kingdom Brain Expression Consortium. An additional k-means clustering step improves the biological features of WGCNA gene co-expression networks. *BMC Syst Biol*. 2017;11(1):47.
75. Kolberg L, Raudvere U, Kuzmin I, Vilo J, Peterson H. gprofiler2 – an R package for gene list functional enrichment analysis and namespace conversion toolset g:Profiler. *F1000Research*. 2020; 9:709.

76. Qiu X, Mao Q, Tang Y, et al. Reversed graph embedding resolves complex single-cell trajectories. *Nat Methods*. 2017; 14(10):979–982.
77. Trapnell C, Cacchiarelli D, Grimsby J, et al. The dynamics and regulators of cell fate decisions are revealed by pseudotemporal ordering of single cells. *Nat Biotechnol*. 2014;32(4):381–386.
78. Xiang X, Piers TM, Wefers B, et al. The Trem2 R47H Alzheimer's risk variant impairs splicing and reduces Trem2 mRNA and protein in mice but not in humans. *Mol Neurodegener*. 2018;13(1):49.
79. Vandesompele J, De Preter K, Pattyn F, et al. Accurate normalization of real-time quantitative RT-PCR data by geometric averaging of multiple internal control genes. *Genome Biol*. 2002; 3(7):RESEARCH0034.
80. Salih DAM, Rashid AJ, Colas D, et al. FoxO6 regulates memory consolidation and synaptic function. *Genes Dev*. 2012;26(24): 2780–2801.
81. Kim-Hellmuth S, Bechheim M, Pütz B, et al. Genetic regulatory effects modified by immune activation contribute to autoimmune disease associations. *Nat Commun*. 2017;8(1):266.
82. Alasoo K, Rodrigues J, Mukhopadhyay S, et al.; HIPSCI Consortium. Shared genetic effects on chromatin and gene expression indicate a role for enhancer priming in immune response. *Nat Genet*. 2018;50(3):424–431.
83. Lambert JC, Ibrahim-Verbaas CA, Harold D, et al.; European Alzheimer's Disease Initiative (EADI). Meta-analysis of 74,046 individuals identifies 11 new susceptibility loci for Alzheimer's disease. *Nat Genet*. 2013;45(12):1452–1458.
84. Kunkle BW, Grenier-Boley B, Sims R, et al.; Genetic and Environmental Risk in AD/Defining Genetic, Polygenic and Environmental Risk for Alzheimer's Disease Consortium (GERAD/PERADES). Genetic meta-analysis of diagnosed Alzheimer's disease identifies new risk loci and implicates Aβ, tau, immunity and lipid processing. *Nat Genet*. 2019;51(3): 414–430.
85. Harwood JC, Leonenko G, Sims R, Escott-Price V, Williams J, Holmans P. Defining functional variants associated with Alzheimer's disease in the induced immune response. *Brain Commun*. 2021;3(2):fcab083.
86. Guerreiro R, Bras J. The age factor in Alzheimer's disease. *Genome Med*. 2015;7:106.
87. Ou M, Zhu J, Ji P, et al. Risk factors of severe cases with COVID-19: A meta-analysis. *Epidemiol Infect*. 2020;148:e175.
88. Krasemann S, Madore C, Cialic R, et al. The TREM2-APOE pathway drives the transcriptional phenotype of dysfunctional microglia in neurodegenerative diseases. *Immunity*. 2017;47(3): 566–581.e9.
89. Griciuc A, Patel S, Federico AN, et al. TREM2 acts downstream of CD33 in modulating microglial pathology in Alzheimer's disease. *Neuron*. 2019;103(5):820–835.e7.
90. Scott-Hewitt N, Perrucci F, Morini R, et al. Local externalization of phosphatidylserine mediates developmental synaptic pruning by microglia. *EMBO J*. 2020;39(16):e105380.
91. Györffy BA, Kun J, Török G, et al. Local apoptotic-like mechanisms underlie complement-mediated synaptic pruning. *Proc Natl Acad Sci U S A*. 2018;115(24):6303–6308.
92. Schwartz SL, Conn GL. RNA regulation of the antiviral protein 2′-5′-oligoadenylate synthetase. *WIREs RNA*. 2019;10(4):e1534.
93. Schwartz SL, Park EN, Vachon VK, Danzy S, Lowen AC, Conn GL. Human OAS1 activation is highly dependent on both RNA sequence and context of activating RNA motifs. *Nucleic Acids Res*. 2020;48(13):7520–7531.
94. Schmiedel BJ, Singh D, Madrigal A, et al. Impact of genetic polymorphisms on human immune cell gene expression. *Cell*. 2018;175(6):1701–1715.e16.
95. Kuksa PP, Lui C-L, Fu W et al. Alzheimer's disease variant portal (ADVP): A catalog of genetic findings for Alzheimer's disease. *medRxiv*. [Preprint] doi:10.1101/2020.09.29.20203950
96. Broce IJ, Tan CH, Fan CC, et al. Dissecting the genetic relationship between cardiovascular risk factors and Alzheimer's disease. *Acta Neuropathol*. 2019;137(2):209–226.
97. COVID-19 Host Genetics Initiative. Mapping the human genetic architecture of COVID-19. *Nature*. Published online 8 July 2021. doi:10.1038/s41586-021-03767-x
98. Klaassen K, Stankovic B, Zukic B, et al. Functional prediction and comparative population analysis of variants in genes for proteases and innate immunity related to SARS-CoV-2 infection. *Infect Genet Evol*. 2020;84:104498.
99. Tessier M-C, Qu H-Q, Fréchette R, et al. Type 1 diabetes and the OAS gene cluster: Association with splicing polymorphism or haplotype? *J Med Genet*. 2006;43(2):129–132.
100. Cagliani R, Fumagalli M, Guerini FR, et al. Identification of a new susceptibility variant for multiple sclerosis in OAS1 by population genetics analysis. *Hum Genet*. 2012;131(1):87–97.
101. Bonnevie-Nielsen V, Field LL, Lu S, et al. Variation in antiviral 2′,5′-oligoadenylate synthetase (2′5′AS) enzyme activity is controlled by a single-nucleotide polymorphism at a splice-acceptor site in the OAS1 gene. *Am J Hum Genet*. 2005;76(4): 623–633.
102. He J, Feng D, de Vlas SJ, et al. Association of SARS susceptibility with single nucleic acid polymorphisms of OAS1 and MxA genes: A case-control study. *BMC Infect Dis*. 2006;6:106.
103. Randolph HE, Mu Z, Fiege JK, et al. Single-cell RNA-sequencing reveals pervasive but highly cell type-specific genetic ancestry effects on the response to viral infection. *bioRxiv*. [Preprint] doi:10.1101/2020.12.21.423830
104. Zeberg H, Pääbo S. A genomic region associated with protection against severe COVID-19 is inherited from Neandertals. *Proc Natl Acad Sci U S A*. 2021;118:e2026309118.
105. Liddelow SA, Guttenplan KA, Clarke LE, et al. Neurotoxic reactive astrocytes are induced by activated microglia. *Nature*. 2017; 541(7638):481–487.
106. Zheng H, Liu C-C, Atagi Y, et al. Opposing roles of the triggering receptor expressed on myeloid cells 2 and triggering receptor expressed on myeloid cells-like transcript 2 in microglia activation. *Neurobiol Aging*. 2016;42:132–141.
107. Owens R, Grabert K, Davies CL, et al. Divergent neuroinflammatory regulation of microglial TREM expression and involvement of NF-κB. *Front Cell Neurosci*. 2017;11:56.
108. Zhou J, Yu W, Zhang M, Tian X, Li Y, Lü Y. Imbalance of microglial TLR4/TREM2 in LPS-treated APP/PS1 transgenic mice: A potential link between Alzheimer's disease and systemic inflammation. *Neurochem Res*. 2019;44(5):1138–1151.
109. Liu W, Taso O, Wang R, et al. Trem2 promotes anti-inflammatory responses in microglia and is suppressed under pro-inflammatory conditions. *Hum Mol Genet*. 2020;29(19):3224–3248.
110. Moradi Majd R, Mayeli M, Rahmani F. Pathogenesis and promising therapeutics of Alzheimer disease through eIF2α pathway and correspondent kinases. *Metab Brain Dis*. 2020;35(8):1241–1250.
111. De Schepper S, Crowley G, Hong S. Understanding microglial diversity and implications for neuronal function in health and disease. *Dev Neurobiol*. 2021;81(5):507–523.
112. Zhang Z, Zhang Z-Y, Schittenhelm J, Wu Y, Meyermann R, Schluesener HJ. Parenchymal accumulation of CD163+ macrophages/microglia in multiple sclerosis brains. *J Neuroimmunol*. 2011;237(1-2):73–79.
113. Pey P, Pearce RKB, Kalaitzakis ME, Griffin WST, Gentleman SM. Phenotypic profile of alternative activation marker CD163 is different in Alzheimer's and Parkinson's disease. *Acta Neuropathol Commun*. 2014;2:21.

114. Dvir-Szternfeld R, Castellani G, Arad M, et al. TREM2-independent neuroprotection is mediated by monocyte-derived macrophages in a mouse model of Alzheimer's disease. *Nat Res*. 2021.
115. Wang F, Kream RM, Stefano GB. Long-term respiratory and neurological sequelae of COVID-19. *Med Sci Monit*. 2020;26: e928996.
116. Wood ER, Bledsoe R, Chai J, et al. The role of phosphodiesterase 12 (PDE12) as a negative regulator of the innate immune response and the discovery of antiviral inhibitors. *J Biol Chem*. 2015;290(32):19681–19696.
117. Kingwell E, Leray E, Zhu F, et al. Multiple sclerosis: Effect of beta interferon treatment on survival. *Brain*. 2019;142(5):1324–1333.
118. Wang N, Zhan Y, Zhu L, et al. Retrospective multicenter cohort study shows early interferon therapy is associated with favorable clinical responses in COVID-19 patients. *Cell Host Microbe*. 2020;28(3):455–464.e2.
119. Davoudi-Monfared E, Rahmani H, Khalili H, et al. A randomized clinical trial of the efficacy and safety of interferon β-1a in treatment of severe COVID-19. *Antimicrob Agents Chemother*. 2020;64(9):e01061–20.